Available online at www.sciencedirect.com
ScienceDirect
Polymer 48 (2007) 2644–2648
polymer
www.elsevier.com/locate/polymer

The inhibition effect of 20(*S*)-Protopanaxadiol (PPD) and Ginsenoside Rh2 for CYP2C9 and CYP3A4

Yuan Yao [a], Wei-wei Han [a], Yi-han Zhou [a], Ze-sheng Li [a,*], Qiang Li [b], Xiao-yan Li [b], Xiao-yan Chen [b], Da-fang Zhong [b,**]

[a] *Institute of Theoretical Chemistry, State Key Laboratory of Theoretical and Computational Chemistry, Jilin University, Changchun 130023, PR China*
[b] *Center for Drug Metabolism Research, Shanghai Institute of Materia Medica, Chinese Academy of Sciences, Shanghai 201203, PR China*

Received 14 December 2006; received in revised form 28 February 2007; accepted 28 February 2007
Available online 7 March 2007

Abstract

With the aid of the automated molecular docking, the inhibition effect of 20(*S*)-Protopanaxadiol (PPD) and Ginsenoside Rh2 for CYP2C9 and CYP3A4, respectively, were studied by InsightII/Affinity program and the docking complexes were analyzed by InsightII/Ludi program. The results indicate that PPD is a competitive inhibitor for CYP2C9 but a poor inhibitor for CYP3A4, Rh2 is a noncompetitive inhibitor for CYP3A4, but a poor inhibitor for CYP2C9. Hydrophobic PPD is stabilized in the center of the substrate-binding regions of CYP2C9 by hydrogen bond and has strong interactions with heme and the key residues in active site which play important role for binding the substrate. Theoretical K_i value was calculated to be 26.7 μM by using Ludi score 457 of CYP2C9–PPD complex. As hydrophilic Rh2 is away from the substrate-binding regions of CYP3A4, it has very weak interactions with the key residues in the active site. But the docking of Rh2 makes the conformation of CYP3A4 to change, including the position of a key residue Ser119 that leads to a decrease in catalytic activity. Theoretical K_i value is 102.8 μM by using Ludi score 398 of CYP3A4–Rh2 complex. The theoretical results are in well agreement with the experimental results.

Keywords: Cytochrome P450s; Docking; Competitive inhibition

1. Introduction

Cytochrome P450s (CYPs) are very important superfamily of biotransformation enzymes that are involved in oxidative metabolism of a wide variety of endogenous and exogenous compounds [1–3]. CYP2C9 is responsible for the metabolic clearance of a wide variety of the therapeutic agents, estimated up to 16% of drugs used in current clinic [4]. CYP3A4 is also known to have broad substrate specificity and metabolize more than 50% of drugs in current clinical used [3,5].

Ginseng, as a crude drug and a traditional medicine, is frequently used and taken orally in Asian countries. It was reported to possess various pharmacological and physiological effects, such as antioxidation [6], antistress [7], immunostimulation [8], anticancer [9], stimulative effects on the central nervous system [10] and pleiotropic antitumour properties [9,11]. Attele et al. reported that ginsenosides are the major active ingredients of ginseng [12]. 20(*S*)-Protopanaxadiol (PPD) is one of the metabolites of ginsenosides from *Panax ginseng* [13]. Ginsenoside Rh2 is one of the active components of ginseng [14]. The structures and Connolly surfaces of them are shown in Fig. 1. The two compounds were reported to exhibit anticancer activity to inhibit the proliferation of cancer cell and induce the apoptosis of cancer cell [11,15].

Numerous people in many countries have taken ginseng or its derived products, however, little is known about the interactions between ginseng and prescription drugs. Therefore, it is necessary to evaluate whether ginseng and its active components exhibit the potential to exert influence on metabolic

* Corresponding author. Tel.: +86 431 88498960; fax: +86 431 88498026.
** Corresponding author. Tel./fax: +86 21 50800738.
E-mail addresses: zeshengli@mail.jlu.edu.cn (Z.-s. Li), zhongdf@china.com (D.-f. Zhong).

0032-3861/$ - see front matter © 2007 Elsevier Ltd. All rights reserved.
doi:10.1016/j.polymer.2007.02.069

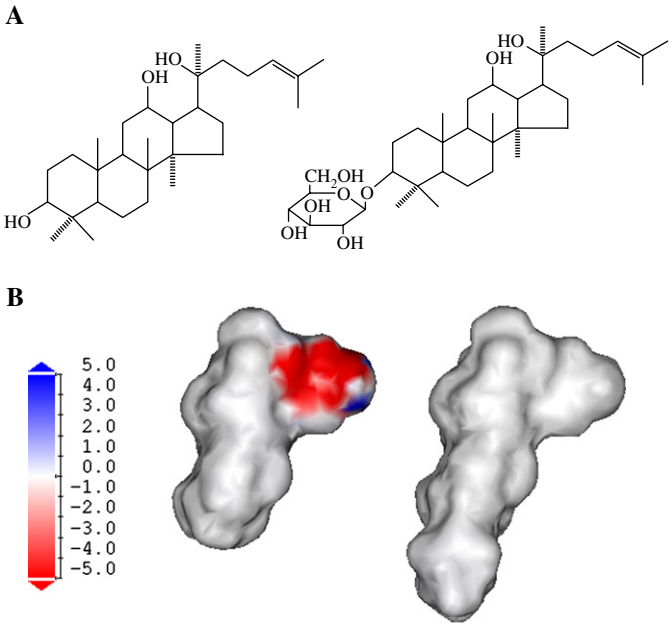

Fig. 1. The structures and the Connolly surfaces by the analysis of the electrostatic surface potential of PPD (left) and Rh2 (right) in part A and part B, respectively.

enzymes. In the present study, the automated molecular docking is performed to investigate the inhibition of the two compounds for CYP2C9 and CYP3A4.

2. Theory and methods

All studies were performed on SGI O3800 workstation.

2.1. Binding-site analysis

The binding-site module [16] is a suite of programs in InsightII software package for identifying and characterizing protein active sites, binding sites, and functional residues from protein structures and multiple sequence alignments. In this study, ActiveSite-Search was used to identify protein active sites and binding sites by locating cavities in CYP structures. When the search was completed, the largest site was automatically displayed on the structure and the other two sites are also obtained by using Asite-Display. The results were used to guide the protein–ligand docking experiments.

2.2. Flexible docking

Affinity [17], which uses a combination of Monte Carlo type and Simulated Annealing (SA) method, is a suite of programs for automatically docking a ligand to a receptor in InsightII software package. A key feature is that the "bulk" of the receptor, defined as atoms not in the binding site specified, keeps rigid during the docking process, while the binding-site atoms and ligand atoms are movable. By means of the 3D structures of PPD and Rh2 which are built and optimized through the InsightII/Builder program, the automated molecular docking was performed by using docking program, Affinity. The potential function of the complexes was assigned by using the consistent-valence force field (CVFF) and non-bonding interaction was dealt with the cell multipole approach. To account the solvent effect, the centered enzyme–ligand complexes were solvated in a sphere of TIP3P water molecules with radius 10 Å. This provides 10 structures from SA docking, and clustered according to RMS deviation. Finally, the docked complex of the receptor with the ligand was selected by the criteria of interacting energy combined with the geometrical matching quality.

2.3. Ludi score

Ludi method [18] is useful for *de novo* design of ligands for proteins and inhibitors for enzymes. This program screens a large number of compounds and analyzes a geometrical fit of given chemicals into the binding site. It also can determine other good binding properties such as hydrogen bonds, lipophilic interactions, ionic interactions, and acylic interactions. In general, a higher Ludi score represents a higher affinity and stronger binding of a ligand to the receptor. The relation between Ludi score and dissociation constant K_i (M) can be expressed as:

$$\text{Ludi score} = -100 \log K_i \quad (1)$$

3. Results and discussion

3.1. Identification of binding region

InsightII/binding-site module is used to search the substrate-binding regions of CYP2C9 (PDB code 1R9O [19]) and CYP3A4 (PDB code 1TQN [20]). The largest binding regions which we obtained are in good agreement with the known hydrophobic active sites of 1R9O [19] and 1TQN [20,21].

3.2. Docking of PPD to CYP2C9 and CYP3A4

PPD has the common hydrophobic head as presented in Fig. 1. The CYP2C9–PPD, CYP3A4–PPD complexes are generated by using the InsightII/Affinity module. In docking complexes, PPD is stabilized in the center of the binding regions of CYP2C9 and CYP3A4 by hydrogen bond and hydrophobic interactions. As is well known, hydrogen bond plays an important role for structure and function of biological molecules, especially for the enzyme catalytic reaction. In the CYP2C9–PPD complex, one hydrogen atom of PPD is hydrogen bonded to Asn484 and only one hydrogen bond is formed. In the CYP3A4–PPD complex, the same hydrogen atom of PPD is hydrogen bonded to Ser119 and only one hydrogen bond is formed. These hydrogen bonds are helpful to stabilize the CYP2C9–PPD, CYP3A4–PPD complexes, respectively.

The interaction energy analysis indicates that the CYP2C9–PPD complex has large favorable total interaction

energy of −64.87 kcal/mol, van der Waals and electrostatic energies are −58.23 and −6.64 kcal/mol, respectively. CYP3A4–PPD complex has favorable total interaction energy of −37.35 kcal/mol, van der Waals and electrostatic energies are −29.73 and −7.61 kcal/mol, respectively. The lower total interaction energy means that the higher affinity exists between inhibitor and enzymes. The higher Ludi score 457 of CYP2C9–PPD complex means a higher affinity and stronger binding of PPD to CYP2C9. The Ludi score 298 of CYP3A4–PPD complex which is smaller than 300 means not good affinity and stable binding of PPD to CYP3A4. The results of the interaction energy analysis and Ludi score suggest that PPD is a good inhibitor for CYP2C9 but not for CYP3A4. Thus, the complex of CYP3A4–PPD will be ignored in later analysis.

The superposition of the binding 3D conformation within the active site of CYP2C9–PPD complex is shown in Fig. 2. To determine the key residues in the CYP2C9–PPD complexes, the interaction energies of PPD with each of the residues in the active site of CYP2C9 are calculated. Significant binding-site residues in the models are identified by the total interaction energy. In general, if the interaction energy between the residues and the ligand is lower than −1 kcal/mol, those residues are considered to be important in the complex. Table 1 gives the interaction energies including the total, van der Waals and electrostatic energies with the total energy lower than −2 kcal/mol for all residues which are considered to be more important. The attractive interaction of electrostatic or van der Waals between heme and PPD is very important for PPD binding orientation and absolutely necessary for the hydroxylation mechanism. Through interaction energy analysis, one can see from Table 1 that heme, Gly296, Leu208, Ile205, Asn474, Phe476 and Asn204 of CYP2C9 are the most important anchoring residues for binding with PPD because they have strong van der Waals and electrostatic interactions with PPD. To our knowledge, Phe476 [22], Asp293 [23] and Arg108 [24] have been identified by experiments to be the important residues for binding and stabilizing the substrate.

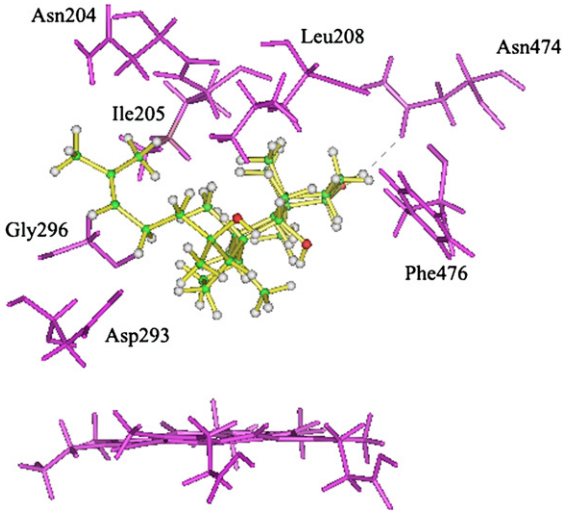

Fig. 2. 3D structure of CYP2C9–PPD complex. PPD is rendered as ball and stick, heme and the residues are rendered as stick. One hydrogen bond is formed between PPD and Asn474. The bond distance is 2.37 Å and the bond angle is 159.80°.

Table 1
The total energy (E_{total}), van der Waals energy (E_{vdw}), and electrostatic energy (E_{ele}) between PPD and individual residues in CYP2C9–PPD complex ($E_{total} < -2.00$ kcal/mol)

Residues	E_{vdw} (kcal/mol)	E_{ele} (kcal/mol)	E_{total} (kcal/mol)
Enzyme	−58.235	−6.635	−64.870
HEME	−16.253	−0.132	−16.385
Gly296	−4.329	−1.106	−5.435
Leu208	−4.174	−0.280	−4.455
Ile205	−3.873	−0.230	−4.103
Asn474	−1.069	−2.763	−3.832
Phe476	−4.125	0.832	−3.293
Asn204	−2.899	−0.105	−3.004
Asp293	−2.650	−0.120	−2.770
Leu362	−2.490	0.137	−2.353
Phe100	−1.782	−0.418	−2.200
Phe114	−1.757	−0.444	−2.200
Arg108	−2.154	0.062	−2.092

Thus, we think that PPD is a competitive inhibitor for CYP2C9. Firstly, PPD is stabilized in the center of active site of CYP2C9, so that it can affect the substrates entering into the active site of CYP2C9 and closing to Fe atom in heme. Secondly, from the energy, PPD has strong interactions with heme and some important residues in the active site of CYP2C9 so that CYP2C9 cannot bind the substrates firmly and strongly and cannot catalyze them effectively. The theoretical value of dissociation constant K_i of PPD to CYP2C9 is calculated to be 26.7 μM by using Eq. (1). Our theoretical results are in good agreement with the experimental results by some of the present authors that PPD exhibits competitive inhibition with K_i value of 35.8 μM and IC_{50} value of 27.32 μM for CYP2C9, but IC_{50} value > 450 μM for CYP3A4.

3.3. Docking of Rh2 to CYP2C9 and CYP3A4

The automated molecular docking was performed by using InsightII/Affinity program. Because Rh2 is hydrophilic it cannot be stabilized in the hydrophobic active sites of CYP2C9 and CYP3A4. Thus, we choose another active site which is away from the hydrophobic active sites by using InsightII/binding-site module and get the CYP2C9–Rh2, CYP3A4–Rh2 complexes successfully. There are three hydrogen bonds formed between Rh2 and CYP3A4, but no hydrogen bond formed between Rh2 and CYP2C9. The hydrogen bond interactions stabilize the docking complex so that less hydrogen bond leads to less stabilization for Rh2 in the active site of CYP2C9. The CYP3A4–Rh2 complex has large favorable total interaction energy of −68.97 kcal/mol, van der Waals and electrostatic energies are −56.26 and −12.72 kcal/mol, respectively. And CYP2C9–Rh2 complex has favorable total interaction energy of −54.00 kcal/mol, van der Waals and electrostatic energies are −50.67 and −3.33 kcal/mol, respectively. The Ludi score 398 of CYP3A4–Rh2 complex means a higher affinity and stronger binding of Rh2 to CYP3A4.

The Ludi score 274 of CYP2C9–Rh2 complex which is smaller than 300 means that the affinity and binding of Rh2 to CYP2C9 are not strong compared with CYP3A4–Rh2 complex. Thus, by analyzing hydrogen bonding, Ludi score, and the interaction energies, we think that Rh2 is a good inhibitor for CYP3A4 but not for CYP2C9. Thus, the analysis of CYP2C9–Rh2 complex will be ignored below. The superposition of the binding 3D conformation within the active site of CYP3A4–Rh2 complex is shown in Fig. 3. Through interaction energy analysis, it is found from Table 2 that Asp270, Phe137, Leu274, Lys141 and Phe302 of CYP3A4 are the most important anchoring residues for binding with Rh2 because they have strong van der Waals and electrostatic interactions with Rh2.

Thus, we think that Rh2 is a noncompetitive inhibitor for CYP3A4. Firstly, Rh2 is not located in the active site of CYP3A4, but located away from it so that the substrate can enter into the active site smoothly and close to the Fe atom of heme. Secondly, an overlap of Cα of the CYP3A4 and CYP3A4–Rh2 complex in Fig. 4 shows that the docking of Rh2 causes a conformational change of residues Lys115-Ile120, Lys127-Thr138, Ser186-Phe189 and Lys266-Ser281. Especially, Ser119 is an important residue for binding the substrate [21] so that the change leads to a decrease in catalytic activity. The value of a dissociation constant K_i of Rh2 to CYP3A4 is 102.8 μM which is estimated theoretically by means of Eq. (1). Our theoretical results are in good agreement with the experimental results by some of the present authors

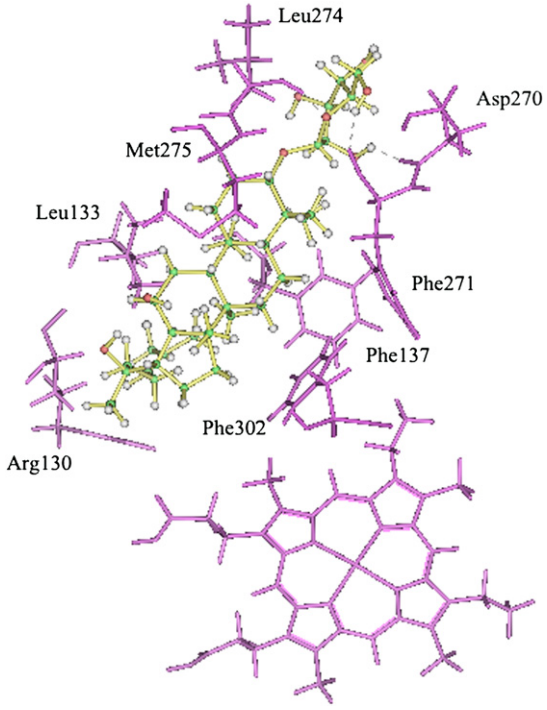

Fig. 3. 3D structure of CYP3A4–Rh2 complex. Rh2 is rendered as ball and stick, heme and the residues are rendered as stick. Three hydrogen bonds are formed between Rh2 with Asp270, Phe271 and Leu274. The bond distances are 2.37, 1.73 and 2.24 Å, the bond angles are 138.86, 151.05 and 147.27°, respectively.

Table 2
The total energy (E_{total}), van der Waals energy (E_{vdw}), and electrostatic energy (E_{ele}) between Rh2 and individual residues in the CYP3A4–Rh2 complex ($E_{total} < -2.00$ kcal/mol)

Residue	E_{vdw} (kcal/mol)	E_{ele} (kcal/mol)	E_{total} (kcal/mol)
Enzyme	−56.257	−12.717	−68.974
Asp270	−3.700	−3.341	−7.041
Phe137	−5.920	−0.106	−6.025
Leu274	−2.532	−2.730	−5.262
Lys141	−4.011	−0.844	−4.855
Phe302	−4.860	0.130	−4.729
Met275	−4.165	0.362	−3.803
Arg130	−3.852	0.265	−3.587
Thr136	−3.340	0.151	−3.189
Leu133	−2.209	−0.876	−3.085
Gln273	−1.609	−1.123	−2.732
His267	−1.669	−1.035	−2.703
Leu272	−2.273	−0.276	−2.549
Leu290	−2.170	−0.163	−2.333
Ile443	−2.186	−0.090	−2.276

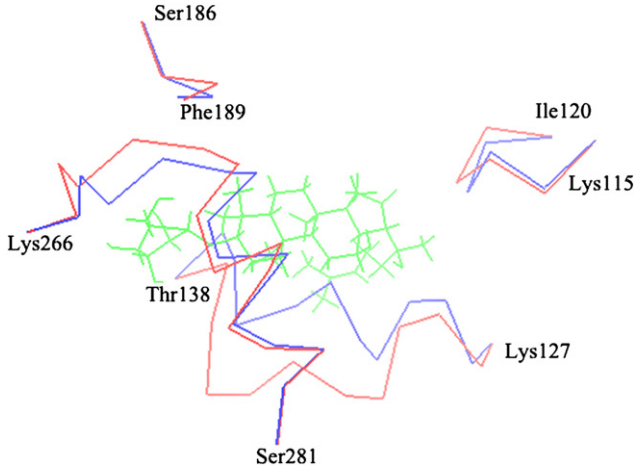

Fig. 4. An overlap of Cα of the CYP3A4 and CYP3A4–Rh2 complex. CYP3A4 is represented by blue color, CYP3A4–Rh2 complex is represented by red color, Rh2 is represented by green color. (For interpretation of the references to color in this figure legend, the reader is referred to the web version of this article.)

which show that Rh2 exhibits noncompetitive inhibition with K_i value of 115.5 μM and IC_{50} value of 180.56 μM for CYP3A4, but poor inhibition for CYP2C9 with IC_{50} values of 329.03 μM.

4. Conclusion

In this paper, the automated molecular docking studies were performed by InsightII/Affinity program to explore inhibition effect of 20(*S*)-Protopanaxadiol (PPD) and Ginsenoside Rh2 for CYP2C9 and CYP3A4, respectively. With the analysis of hydrogen bond, interactive energy and Ludi score, we suggest that PPD is a competitive inhibitor for CYP2C9 but a poor inhibitor for CYP3A4, hydrophobic PPD is stabilized in the center of the substrate-binding regions of CYP2C9 by hydrogen bond and has strong interactions with heme and the key

residues in active site which play very important role for binding the substrate. Theoretical K_i value is calculated to be 26.7 μM by using Ludi score 457 of CYP2C9–PPD complex. Hydrophilic Rh2 is a noncompetitive inhibitor for CYP3A4, but a poor inhibitor for CYP2C9. Rh2 is stabilized away from the substrate-binding regions of CYP3A4 and has very weak interactions with the key residues in the active site. The docking of Rh2 causes a conformational change of CYP3A4, including a key residue Ser119 that leads to a decrease in catalytic activity. Theoretical K_i value is 102.8 μM by using Ludi score 398 of CYP3A4–Rh2 complex. The theoretical results are in good agreement with the experimental results.

Acknowledgments

This work is supported by the National Science Foundation of China (20333050, 20673044), Doctor Foundation by the Ministry of Education, and Foundation for University Key Teacher by the Ministry of Education, Key subject of Science and Technology by the Ministry of Education of China, and Key subject of Science and Technology by Jilin Province.

References

[1] Denisov IG, Makris TM, Sligar SG, Schlichting I. Chem Rev 2005; 105:2253.
[2] Nebert DW, Gonzalez FJ. Annu Rev Biochem 1987;56:945.
[3] Guengerich FP. Chem Res Toxicol 2001;14:611.
[4] Schwarz UI. Eur J Clin Invest 2003;33:23.
[5] Wrighton SA, Schuetz EG, Thummel KE, Shen DD, Korzekwa KR, Watkins PB. Drug Metab Rev 2000;32:339.
[6] Zhang D, Yasuda T, Yu Y, Zheng P, Kawabata T, Ma Y, et al. Free Radical Biol Med 1996;20:145.
[7] Wang L, Lee TF. Planta Med 2000;66:144.
[8] Shin JY, Song JY, Yun YS, Yang HO, Rhee DK, Pyo S. Immunopharmacol Immunotoxicol 2002;24:469.
[9] Shibata S. J Korean Med Sci 2001;16:28.
[10] Nishijo H, Uwano T, Zhong YM, Ono T. J Pharm Sci 2004;95:145.
[11] Yun TK. Mutat Res 2003;523–524:63.
[12] Attele AS, Wu JA, Yuan CS. Biochem Pharmacol 1999;58:1685.
[13] Lee SH, Seo GS, Ko G, Kim JB, Sohn DH. Planta Med 2005;12:1167.
[14] Park EK, Choo MK, Oh JK, Ryu JH, Kim DH. Biol Pharm Bull 2004;27:433.
[15] Popovich DG, Kitts DD. Arch Biochem Biophys 2002;406:1.
[16] Binding site analysis user guide. San Diego, USA: Accelrys, Inc.; 1999.
[17] Affinity user guide. San Diego, USA: Accelrys, Inc.; 1999.
[18] Ludi score user guide. San Diego, USA: Accelrys, Inc.; 1999.
[19] Wester MR, Yano JK, Schoch GA, Yang C, Griffin KJ, Stout CD, et al. J Biol Chem 2004;279:35630.
[20] Yano JK, Wester MR, Schoch GA, Griffin KJ, Stout CD, Johnson EF. J Biol Chem 2004;279:38091.
[21] Tanaka T, Okuda T, Yamamoto Y. Chem Pharm Bull 2004;52:830.
[22] Melet A, Jean AP, Lopez-Garcia MP, Marques-Soares C, Jaouen M, Dansette PM, et al. Arch Biochem Biophys 2003;409:80.
[23] Flanagan JU, McLaughlin LA, Paine MJ, Sutcliffe MJ, Roberts GC, Wolf CR. Biochem J 2003;370:921.
[24] Ridderstrom M, Masimirembwa C, Trump-Kallmeyer S, Ahlefelt M, Otter C, Anderson TB. Biochem Biophys Res Commun 2000;270:983.